

Scanning Hall probe microscopy with shear force distance control

Thomas Schweinböck, Dieter Weiss, Martin Lipinski, and Karl Eberl

Citation: [Journal of Applied Physics](#) **87**, 6496 (2000); doi: 10.1063/1.372749

View online: <http://dx.doi.org/10.1063/1.372749>

View Table of Contents: <http://scitation.aip.org/content/aip/journal/jap/87/9?ver=pdfcov>

Published by the [AIP Publishing](#)

Articles you may be interested in

[A scanning Hall probe microscope for large area magnetic imaging down to cryogenic temperatures](#)

Rev. Sci. Instrum. **73**, 3515 (2002); 10.1063/1.1505097

[Scanning Hall probe microscopy on an atomic force microscope tip](#)

J. Vac. Sci. Technol. A **19**, 1769 (2001); 10.1116/1.1379324

[Magnetic detection of cracks by fatigue in mild steels using a scanning Hall-sensor microscope](#)

Rev. Sci. Instrum. **70**, 184 (1999); 10.1063/1.1149563

[Measurement of the stray field emanating from magnetic force microscope tips by Hall effect microsensors](#)

J. Appl. Phys. **82**, 3182 (1997); 10.1063/1.365623

[High-performance low-cost Hall probe measuring head](#)

Rev. Sci. Instrum. **68**, 1465 (1997); 10.1063/1.1147634



Launching in 2016!

The future of applied photonics research is here

AIP | APL
Photonics

Scanning Hall probe microscopy with shear force distance control

Thomas Schweinböck^{a)} and Dieter Weiss

Institut für Experimentelle und Angewandte Physik, Universität Regensburg, D-93040 Regensburg, Germany

Martin Lipinski and Karl Eberl

Max-Planck-Institut für Festkörperforschung, Heisenbergstrasse 1, D-70569 Stuttgart, Germany

We describe a new type of scanning Hall probe microscope operating at room temperature for quantitative and noninvasive measurements of magnetic stray fields. The probe-sample distance is controlled by piezoelectrical detection of the shear forces acting on an oscillating cantilever. The Hall probes are manufactured from prepatterned GaAs wafers overgrown with a GaAs/AlGaAs heterostructure containing a high-mobility two-dimensional electron gas a few ten nm below the surface. The active Hall area is defined by optical and electron-beam lithography with a junction width of $0.6\ \mu\text{m}$ yielding in a resolution of approximately $0.4\ \mu\text{m}$. The Hall coefficient of the sensor at room temperature is $0.23\ \Omega/\text{G}$ with a noise level of $\sim 0.1\ \text{G}/\text{Hz}^{1/2}$. We show measurements of the stray field pattern of bits written on a magnetic hard disk. © 2000 American Institute of Physics. [S0021-8979(00)20008-X]

I. INTRODUCTION

Since the invention of the magnetic force microscope (MFM),¹ several attempts have been made to establish a quantitative and noninvasive method for measuring stray fields in the submicron regime. Among those are scanning SQUID microscopy,² scanning MR heads,³ and scanning Hall probe microscopy (SHPM).^{4,5} SHPM meets both needs since the Hall probe has a very low self-field which could interfere with the sample and the Hall voltage is directly related to the out-of-plane component of the stray field penetrating the sensor. Possible applications of the SHPM are imaging of surface domain structures, inhomogeneous current flow in integrated circuits or vortices in superconducting films.

The first SHPMs presented by Chang *et al.* and Oral *et al.* had a distance control based on a scanning tunneling microscopy (STM)-tip in the vicinity of the Hall junction.^{4,5} In contrast, we employ a piezoelectric distance control based on shear force detection similar to those used for scanning near-field optical microscopes (SNOM).^{6,7} This allows the investigation of nonconducting or not uniformly conducting samples such as patterned magnetic samples or integrated circuits.

II. SAMPLE PREPARATION AND INSTRUMENTATION

We used a commercial Digital Instruments Multimode™ Scanning Probe Microscope with a home-made probe head including the shear force distance control (see Fig. 1). Similar to a technique first presented by Brunner *et al.*⁷ where a glass fiber is mounted between two piezo plates and acts as a resonator for a SNOM, we use a narrow GaAs chip (typically $4\ \text{mm} \times 0.5\ \text{mm} \times 0.4\ \text{mm}$ in size) as a cantilever sandwiched between two piezo plates. The Hall probe is then glued to the front edge of the cantilever. One of the piezo plates is driven by an ac voltage of typically 1000 mV at the cantilever's

resonance frequency (typically in the 20–70 kHz range), while the second piezo detects the amplitude of the cantilever. The amplitude is assumed to be in the 10–100 nm range but definitely smaller than the Hall probe resolution. The amplifying electronics based on fast and low-cost operational amplifiers is described in Ref. 8. We observed Q values of the free oscillating cantilever between 20 and 100.

On approaching the sample surface, the oscillation of the cantilever is damped by shear forces until the amplitude reaches a given setpoint value. The setpoint which controls the sensor-sample distance was adjusted to a value of about 80% of the free amplitude. When feedback is established, Hall voltage and surface topography values are acquired simultaneously and imaged depending on the scanner's x and y coordinate.

The Hall sensors used here were fabricated from GaAs/AlGaAs heterojunctions containing a two-dimensional electron gas (2DEG) 100 nm below the surface. The 2D carrier concentration n was $2.5 \times 10^{11}\ \text{cm}^{-2}$ with a mobility μ of $5000\ \text{cm}^2/\text{Vs}$ at room temperature (RT). In conventional

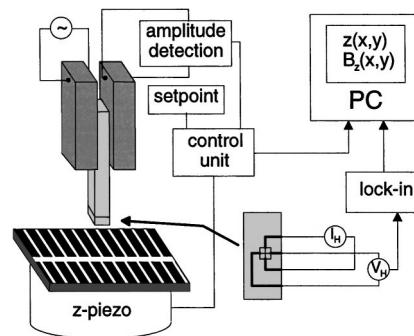


FIG. 1. Schematic view of the shear force detection assembly. The cantilever which is sandwiched between two piezo plates (gray) oscillates at its resonance frequency driven by one of the piezos. The amplitude is detected by the second piezo plate and serves as the control signal for the scanner z -piezo element to maintain constant sensor-sample distance. The Hall voltage, which is proportional to the z component of the local stray field is measured with lock-in technique.

^{a)}Electronic mail: thomas.schweinboeck@physik.uni-regensburg.de

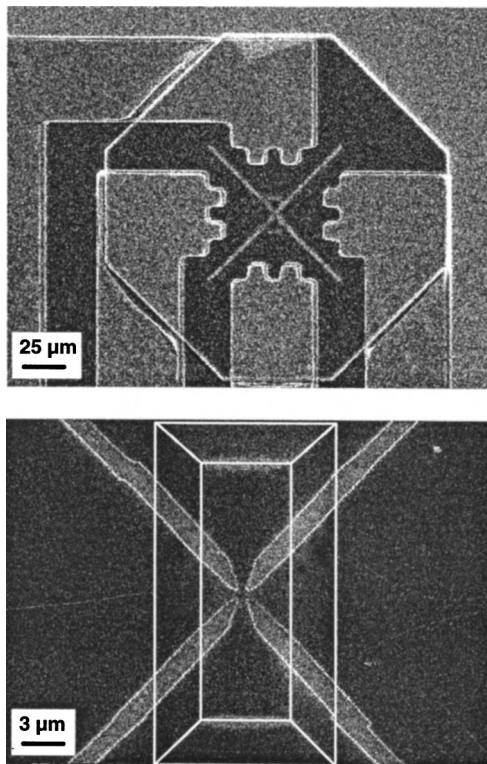


FIG. 2. Scanning electron micrographs of the Hall sensor element. Top image: Hall bar with ohmic contacts and deep mesa etch, the shallow mesa etch defining a $50\text{ }\mu\text{m}$ cross is not visible. Bottom image: Central area of the Hall sensor with the active Hall junction confining on top of the mesa, the white lines highlight the edges of the prepatterned etch structure.

Hall sensors, the ohmic contacts consisting of an alloyed layer of AuGe/Ni, which in our case has a thickness of $\sim 300\text{ nm}$, define the protrusive elements of the device topography. In order to minimize the distance between the surface to be investigated and the 2DEG, we employ a nonplanar 2DEG obtained by overgrowing a prepatterned GaAs substrate. The pattern defined by wet-chemical etching sensitive to the crystallographic directions consists of a mesa having the shape of a cut-off roof with an area of $5 \times 30\text{ }\mu\text{m}^2$ and a height of $1\text{ }\mu\text{m}$. After molecular-beam epitaxy overgrowth, the top area of the structure becomes $8 \times 24\text{ }\mu\text{m}^2$ due to material diffusion during the growing process. Along the long sides of the structure, which are oriented such as to form $(11n)A$ facets (where n has a value ≥ 4), as well as on the top of the structure, which defines again a (001) facet, a high-mobility layer is formed (as described in Ref. 9) leading the electrons to the Hall junction.

The active area is patterned by optical lithography and electron-beam lithography (EBL) as shown in scanning electron micrographs (Fig. 2). First, a deep wet-chemical mesa etch ($\sim 2\text{ }\mu\text{m}$) defines an octagon, on which the cross-like mesa is defined. Ohmic contacts to the 2DEG and metallic interconnections around the chip corner are defined by lift-off technique. Subsequently, the electron gas in the mesa is further confined by EBL and chemically assisted ion beam etching (CAIBE) such that the active Hall junction lies in the center of the overgrown etch structure. The minimum tip-sample distance is therefore only determined by the depth of the 2DEG below the surface, which is about 100 nm . Junction

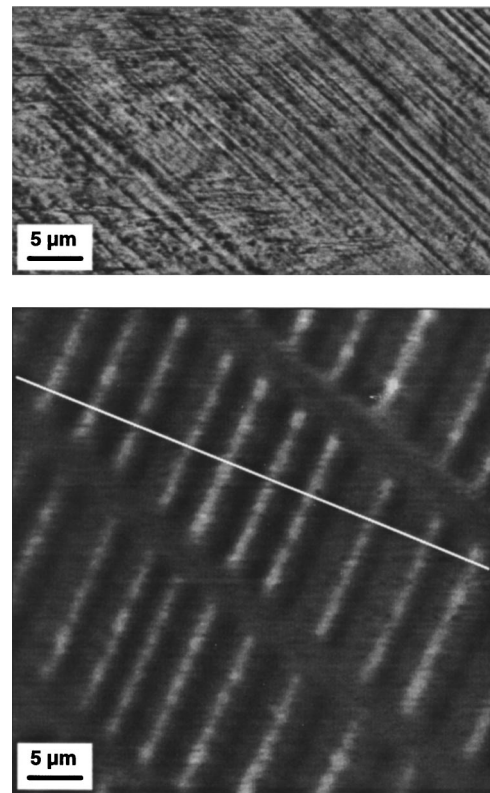


FIG. 3. Cantilever amplitude (top) and Hall signal (bottom) images of a magnetic hard disk. Scanning area is $47 \times 25\text{ }\mu\text{m}^2$ and $47 \times 47\text{ }\mu\text{m}^2$, voltage range is 1.5 mV and $40\text{ }\mu\text{V}$ for the piezo response signal and the Hall signal, respectively.

widths of 600 nm were fabricated resulting in an effective electrical width of $\sim 400\text{ nm}$ due to depletion of carriers at the edges. Current and voltage pads of the Hall sensor were contacted through evaporation of gold leads over the chip edge and ultrasonic bonding on contact pads at the chip side. The spatial resolution of the sensor is approximately defined by the electrical width of the junction. However, Bending and Oral showed that in the diffusive transport regime, which has to be considered at RT, magnetic flux penetrating through the middle of the junction yields in a higher sensitivity than flux at the edges.¹⁰

III. MEASUREMENTS

Measurements in a homogeneous magnetic field between -4000 and 4000 G perpendicular to the 2DEG yield a linear behavior in the Hall voltage, from which a Hall coefficient of $0.23\text{ }\Omega/\text{G}$ at 300 K can be determined. This corresponds to a 2D carrier density of $2.7 \times 10^{11}\text{ cm}^{-2}$. The series resistance of the device is $37\text{ k}\Omega$.

Figure 3 shows a measurement of the stray field pattern of bits written on a commercial magnetic hard disk (storage density $\sim 20\text{ Mbit/in}^2$). The width of the image is $47\text{ }\mu\text{m}$ with 256 pixels per line. The tracks running from the top left to the bottom right are clearly resolved and so are the individual domain walls with a minimum distance of $2\text{ }\mu\text{m}$ representing the bit edges. Figure 4 shows a profile along the line indicated in Fig. 3. The peak-to-peak difference of the Hall voltage is $\sim 19\text{ }\mu\text{V}$, which corresponds to a stray field

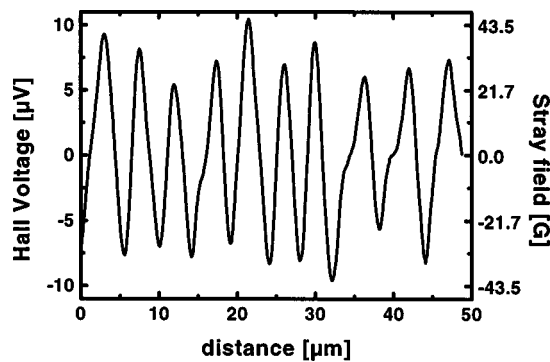


FIG. 4. Line profile along the section indicated in Fig. 3. The measured Hall signal can be directly related to magnetic stray field.

difference of 82 G at a drive current of 1 μA . The magnetic field resolution at a sampling rate of 256 Hz is 0.4 μV or 1.75 G. This results in a signal-to-noise ratio of 47, which is comparable to values of 30–40 typically achieved in MFM measurements of the same sample. If we assume the Johnson noise, $V_n = \sqrt{4k_b T R_s f}$, to be the main noise component of the device, where R_s and f are the series resistance and the measurement bandwidth, respectively, this results in a noise of 0.11 $\text{G/Hz}^{1/2}$ which agrees well with the measured field resolution.

In contrast to previous Hall sensors that had been fabricated on planar 2DEGs with a minimum sensor-sample distance of 400 nm due to ohmic contacts, we achieved a signal enhancement by a factor of 2 and a S/N ratio enhancement by a factor of 5 by using a nonplanar 2DEG.

IV. CONCLUSION

We report on a scanning Hall probe microscope with a shear force distance control working at room temperature with a half-micron resolution and demonstrate the possibility

of imaging individual bits on a magnetic hard disk. S/N ratios measured by this technique are comparable to MFM measurements. We expect that the spatial resolution can be enhanced further (i) by using smaller Hall junctions and (ii) by further reducing the distance between sample and 2DEG.

As a quantitative and noninvasive method for measuring magnetic stray fields, SHPM offers the possibility of imaging soft magnetic materials as well as small magnetic particles. When operated in external magnetic fields, SHPM might develop into a method of probing magnetization reversal loops of individual nanomagnets as in Hall magnetometers (cf., e.g., Refs. 11 and 12).

ACKNOWLEDGMENTS

The authors acknowledge financial support from the Bundesministerium für Bildung, Wissenschaft, Forschung und Technologie (BMBF), Project No. 13N7334/7.

- ¹Y. Martin and H. K. Wickramasinghe, *Appl. Phys. Lett.* **50**, 1455 (1987).
- ²J. R. Kirtley, M. B. Ketchen, K. G. Stawiasz, J. Z. Sun, W. J. Gallagher, S. H. Blanton, and S. J. Wind, *Appl. Phys. Lett.* **66**, 1138 (1995).
- ³R. O'Barr, M. Lederman, and S. Schultz, *J. Appl. Phys.* **79**, 6067 (1996).
- ⁴A. M. Chang, H. D. Hallen, L. Harriot, H. F. Hess, H. L. Loa, J. Kao, R. E. Miller, and T. Y. Chang, *Appl. Phys. Lett.* **61**, 1974 (1992).
- ⁵A. Oral, S. J. Bending, and M. Henini, *Appl. Phys. Lett.* **69**, 1324 (1996).
- ⁶K. Karrai and R. D. Grober, *Appl. Phys. Lett.* **66**, 1842 (1995).
- ⁷R. Brunner, A. Bietsch, O. Hollricher, and O. Marti, *Rev. Sci. Instrum.* **68**, 1769 (1997).
- ⁸H. Brückl, F. Matthes, and G. Reiss, *Appl. Phys. A: Mater. Sci. Process.* **66**, S345 (1998).
- ⁹M. L. Leadbeater, C. L. Foden, J. H. Burroughes, M. Pepper, T. M. Burke, L. L. Wang, M. P. Grimshaw, and D. A. Ritchie, *Phys. Rev. B* **52**, R8629 (1995).
- ¹⁰S. J. Bending and A. Oral, *J. Appl. Phys.* **81**, 3721 (1997).
- ¹¹F. G. Monzon, M. Johnson, and M. L. Roukes, *Appl. Phys. Lett.* **71**, 3087 (1997).
- ¹²A. K. Geim, S. V. Dubonos, J. G. S. Lok, I. V. Grigorieva, J. C. Maan, L. T. Hansen, and P. E. Lindelof, *Appl. Phys. Lett.* **71**, 2379 (1997).